CHAPTER 3

PULSAR OBSERVATIONS WITH THE SINGLE FREQUENCY-CHANNEL RECEIVER

3.1 INTRODUCTION

The sensitivity improvement due to the new tracking facility made it feasible to attempt observation of a few strong pulsars having low dispersion measures (DM). In the first part of this chapter, we will discuss a scheme for such observations, followed by a brief description of the data acquisition system which was built for this purpose. The procedures developed and used for observation, data acquisition, data processing are discussed in detail in the second part. We also present a new criterion for reliable detection. In the third part, we describe the procedures adopted to obtain average pulse profiles, estimates for the average energy per pulse and the amount of interstellar scattering.The prime objective of this work was to make possible detection of pulsar signals and estimation of the

above mentioned average parameters. However, it was thought useful to investigate some possibilities of studying fluctuation spectra and low-frequency variability of pulsar signals using the data obtained during these observations. Our attempts in that direction are reported in the end.

3.2 OBSERVATIONS OF LOW DISPERSION MEASURE PULSARS

3.2.1 The Basic Scheme

In this scheme, we use the existing single frequency channel correlation receiver (Ref. Section 2.2.2), to correlate the outputs of the EW and S arms of the T array. The narrowest available predetection bandwidth of 30 kHz, is close to the optimum bandwidth required for low DM pulsars. Post-detection time-constants $\geq$ 10 milliseconds are possible. Signals from even the strongest of the pulsars will be well buried in the background noise contribution at the detector outputs of our receiver. Thus, it is impossible to detect individual pulses in our observations. However, the introduction of the tracking facility enables us to observe a source over an interval of 42 SEC(δ) minutes. Thus, it is possible to receive a large number of pulses, n_{samp}

(=2520 SEC(δ)/P), from a pulsar at declination 6 and with a period P seconds, in one day. These large number of pulses can be averaged, using standard averaging techniques, to obtain $\sqrt{n_{samp}}$ improvement in the signal-to-noise ratio. With this improvement, it is feasible to observe the average properties of some strong pulsars with low Dispersion Measure.

The required' averaging techniques could be employed on-line by using a suitable hardware system (e.g.[74]) to process the data and to produce a final average at its output. In such a case, the raw data is lost for ever. However, more flexible data processing can be used, if raw data is recorded. Therefore a data logging system was built, to enable recording of raw data onto magnetic tapes using an available incremental mag-tape recorder.

3.2.2 Data Logging System a Design Aspects

The system is designed to enable recording of data from a maximum of 16 analog input channels. A flow chart describing the sequence of operations is shown. in Fig. 3.1. In the mannual mode, the system waits for the end of sidereal minute pulse before initialing the operation, while in the auto mode, the operation starts only when the set start time is reached. The time information is obtained from the Astronomical clock. In the auto mode the operation is controlled by the tracking control system. At the beginning of each new file, a "header"

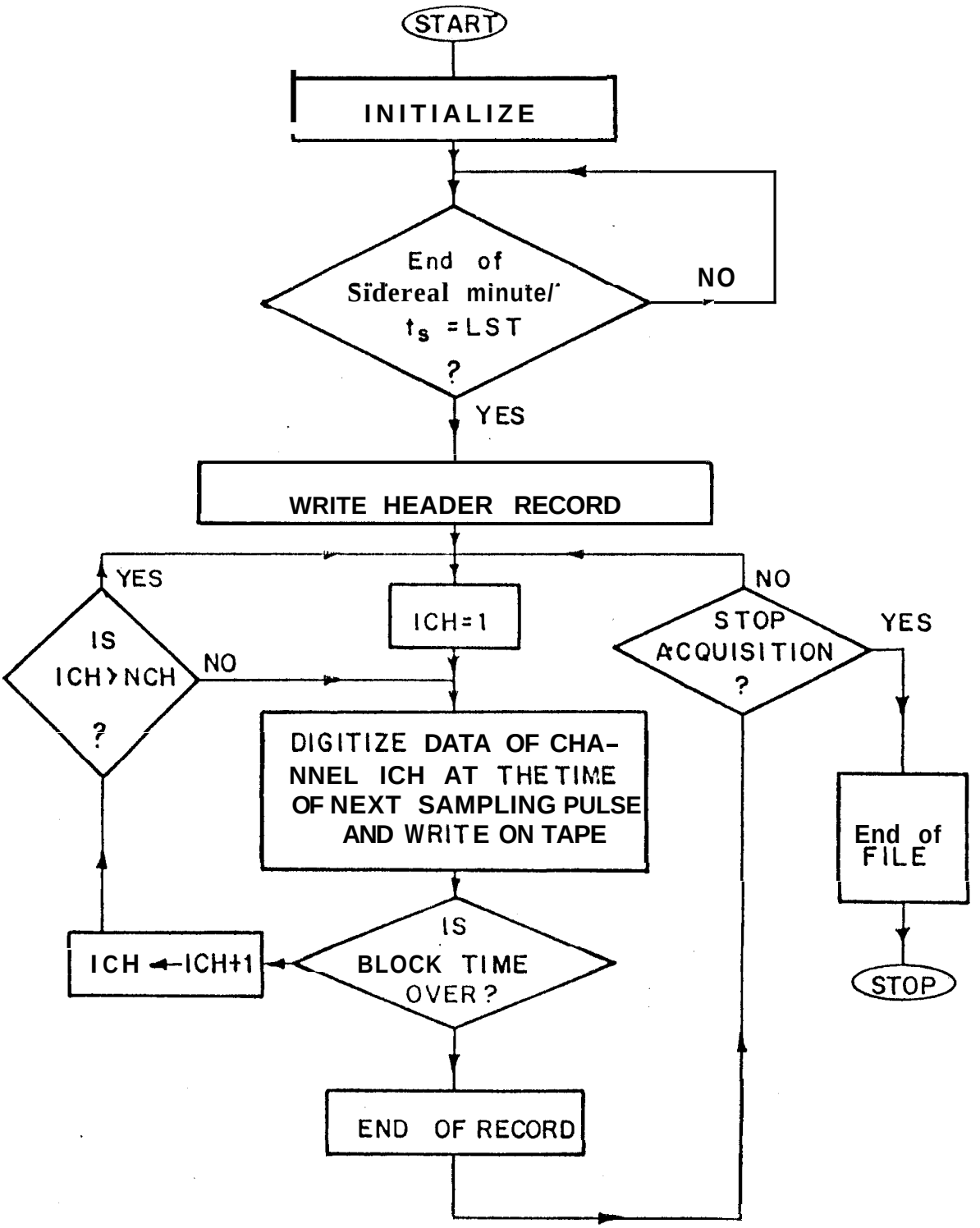

FIG.3.1 A flow chart of the data logger operations.

record is written onto the tape. The header, which is 14 bytes long, consists of a source identifiction code byte, the local sidereal time and Julian day at the start of the acquisition, and the codes indicating the front-panel settings such as sampling rate, number of channels and the input voltage range.

The analog signals for the required number of channels (NCH) are multiplexed, amplified and digitized using an analog-to-digital converter (ADC). The 8-bit digital output from ADC is recorded on to a magnetic tape. The data can be recorded at the fastest rate of 3 milliseconds per sample. This is due to the speed limitation of the magnetic tape drive used. Slower rates are also made available, considering the sampling requirements for continuum observations. The number of channels, the amplifier gain, sampling rate etc. can be selected using suitable settings on the front panel. The data block is terminated every time the EW beam is flipped while tracking or at predetermined intervals of 20 or 60 sidereal seconds.

Fig. 3.2 shows a simplified block diagram of this data logging system.

CMOS digital integrated circuits along with suitable gnalog devices, were used for the hardware realization of the system.

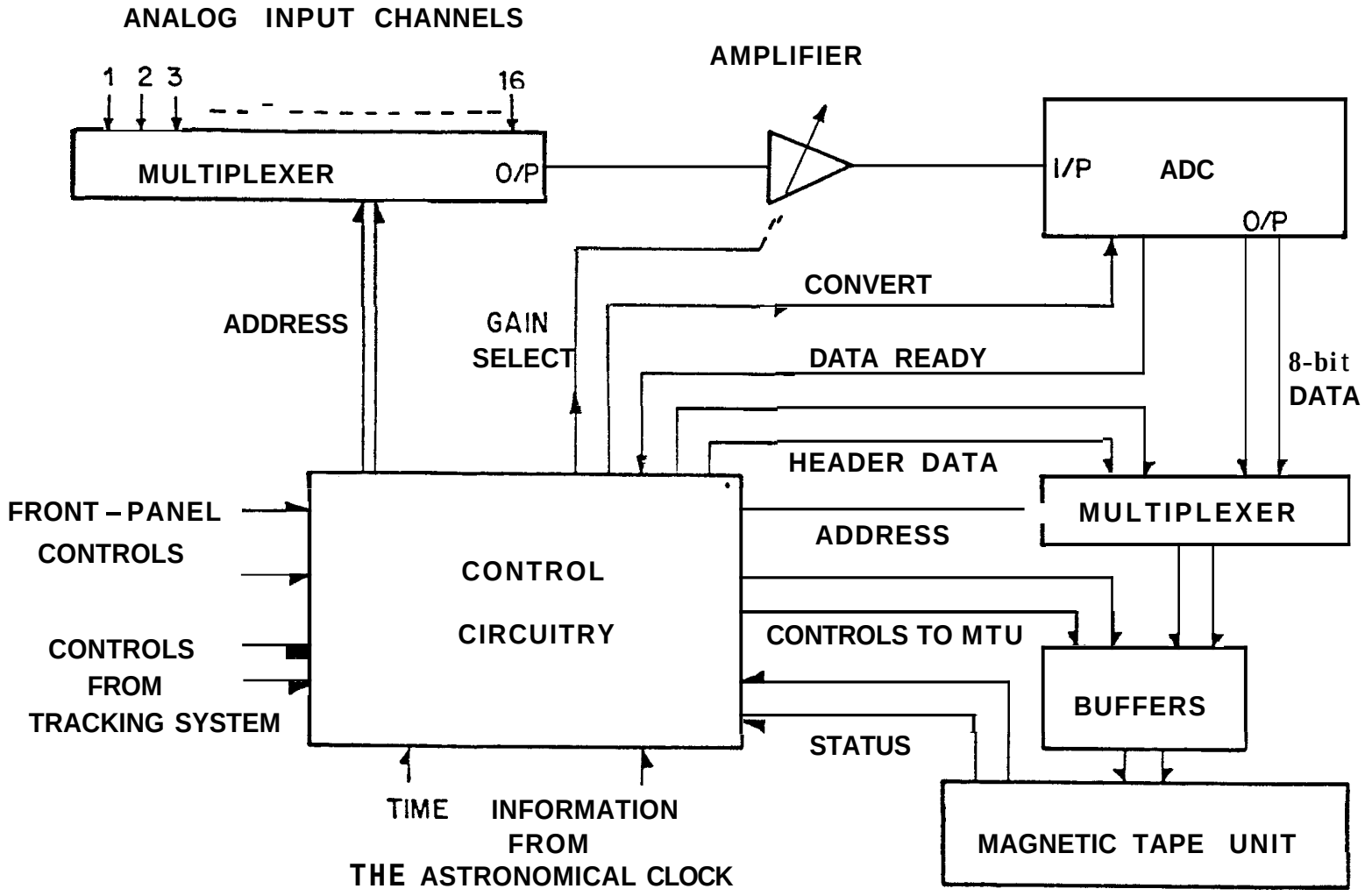

FIG. 3.2 Block diagram of the data logging system.

3.2.3 Observation And Data Acquieition

Following the basic scheme for pulsar observations, we now present the details of the procedures adopted for observation and data acquisition.

The EW and S arm outputs are correlated using the single frequency channel analog correlation receiver. The beams of the two arrays are steered in the N-S direction to the declination of the pulsar. The EW arm is used in the tracking mode. The correlation receiver is used with a predetection bandwidth of 30 KHz and post-detection time-constant of 10/30 milliseconds. In an ideal situation, the SIN correlation beam has zero gain in the direction of the source, while the COS correlation beam has its maximum gain in that direction. In such a case, the SIN correlation could be discarded. However, in practice, due to beam pointing error and ionospheric refraction, the source contribution in the SIN correlation is generally non-zero. This also causes a corresponding reduction in the source contribution and consequent worsening of the signal-to-noise ratio in the COS correlation. Later in this chapter, we present a procedure to partially recover such a loss in the signal-to-noise ratio, using both the correlations. Both the correlations are recorded using the data logging system on to a magnetic tape (NCH=2). The data is sampled at the fastest possible rate, i.e. at a rate of 3 milliseconds per sample. Thus, each of the two correlations

is sampled at intervals of 6 milliseconds. The gain of the amplifier in the data logging system (before the Analog-to-Digital Conversion) is suitably chosen to use the full range of the ADC, thus minimizing the effects of quantization noise. The data records are terminated with an End-of-Record (EOR) mark every time the EW beam is flipped to next position during the tracking. The time taken for writing the EOR mark is more than sufficient for the settling of the tracking phase shifters. Thus, data acquisition is automatically avoided while the beam is flipped.

The gain of the receiver system is monitored at the beginning and at the end of every observation using a calibrated noise source. The arrangement used to enable such measurements is shown in Fig. 3.3.

Using the above mentioned procedure, observations were attempted on 20 known pulsars. These observations were made mostly at night to minimize possible interference due to terrestrial broadcasting signals in the observing band. The relevant parameters for the pulsars and receiver are listed in Table 3.1. Most of these observations were made during 1984 (November) - 1985 (March).

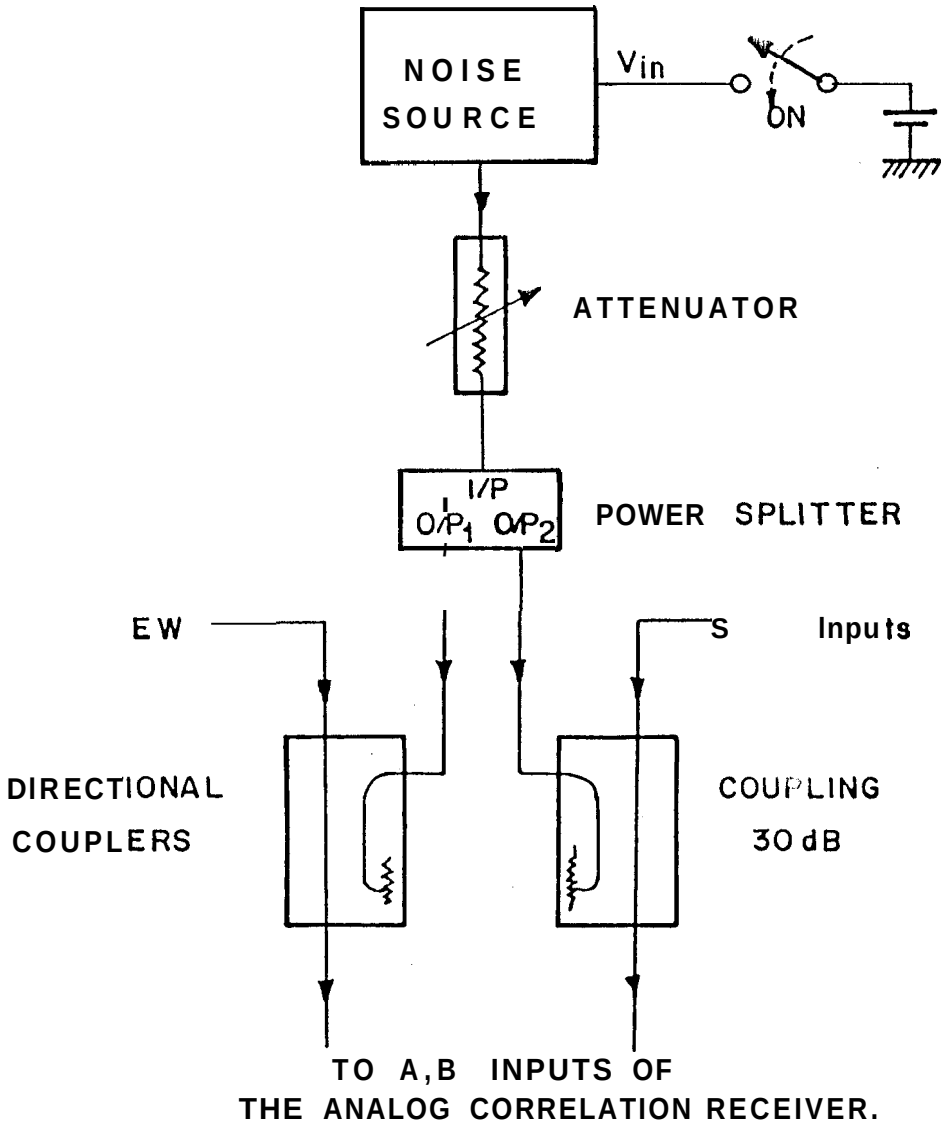

FIG. 3.3 Arrangement for the receiver gain calibration.

TABLE 3.1 RELEVANT PARAMETERS FOR 20 PULSARS

No.	Source Name	Period(s)	DM($cm^{-3}pc$)	n_{samp} *A
1	PSR 0031-07	0.94295078	10.89	2700
2	PSR 0138+59	1.22294827	34.80	4100
3	PSR 0329+54	0.71451866	26.776	6100
4	PSR 0525+21	3.74549703	50.955	700
5	PSR 0628-28	1.24441707	34.36	2300
6	PSR 0655+64	0.19567094	8.9	29700
7	PSR 0809+74	1.29224132	5.757	7300
8	PSR 0823+26	0.53065996	19.4634	5300
9	PSR 0834+06	1.27376417	12.8550	2000
10	PSR 0942-13	0.57026410	12.4	4500
11	PSR 0943+10	1.09770364	15.35	2300
12	PSR 0950+08	0.25306507	2.969	10000
13	PSR 1133+16	1.18791154	4.8479	2200
14	PSR 1237+25	1.38244861	9.296	2000
15	PSR 1508+55	0.73967790	19.599	6000
16	PSR 1919+21	1.33730119	12.4309	2000
17	PSR 1929+10	0.22651715	3.176	11300
18	PSR 2045-16	1.96156688	11.51	1300
19	PSR 2217+47	0.53846739	43.54	7000
20	PSR 2327-20	1.64361966	8.39	1600

Predetection bandwidth 30 KHz

Postdetection time constant 30 msec*

* 10 msec for PSH 0950+08 and 100 msec for PSR 0525+21

** Approximate number of pulses obtainable in one day.

3.2.4 Data Processing

The data processing procedure used here, basically employs the standard "signal averaging technique". This procedure makes use of the known periodic nature of the pulsar signals. If, P is the period of a pulsar, then the samples separated by i.P seconds are averaged, where $i=0,1,\ldots,(n_{samp}-1)$. This reduces the noise fluctuations by a factor of $\sqrt{n_{samp}}$. The procedure developed with this basic idea is described in this section.

First, an apparent period P is calculated as discussed in Appendix I. Using this period P, the number of output bins (NB) is chosen as

$$NB = \text{Int}\,[(P/\Delta Tsamp)+1] \cdot Np \qquad .....(3.1)$$

where, $\Delta Tsamp$ = sampling interval
= 6 milliseconds
Int(X) = interger value of X
Np = number of periods over which averaging is to be performed

and the corresponding binwidth, Δt_{bin} is given by

$$\Delta t_{bin} = P\ (Np/NB) \qquad .....(3.2)$$

It can be seen that Δt_{bin} is less than or equal to $\Delta Tsamp$. In this kind of processing, the data averaging is customarily performed only over a single period stretch. However, here we use Np=2, i.e. perform averaging over a two-period stretch,

for reasons that will be discussed a little later.

The data read from a magnetic tape are demultiplexed into **COS** and **SIN** channels. The data in each of these two channels are processed separately using the following procedure. First, the data is block averaged to obtain a mean value in each data record. One data record cosists of data obtained in one beam position during tracking. The mean values are subtracted from the corresponding samples. The standard deviation in each record is also estimated. The time t, measured with respect to the starting time of acquisition, corresponding to each sample is obtained knowing the beam flipping time (BFT), record number, sampling interval and the sample number. This time , in general, can be written as

$$t = N_S[\ P.Np] + \Delta t_{bin}\ [I + \Delta I] \qquad .....(3.3)$$

where N_S = integral number of Np-period stretches

I = integral number of bins in the fraction of the Np-period stretch ,such that $0 \leq I \leq (NB-1)$

ΔI = fraction of the bin

If one uses synchronous sampling (i.e. $\Delta t_{bin} = \Delta Tsamp$), then ΔI would be identically zero and the sample would be added in the (I)th bin. However, the situation is slightly complicated in the case of asynchronous sampling as is the

present case. If the sample is added to the (I)th or (I+1)th bin depending on whether ΔI is (0.5 or $\geq$0.5, the resultant profile would be smeared over Δt_{bin}. We avoid such smearing by using linear interpolation to add the sample value with suitable weights in both ,the (I)th and (I+1)th, bins as given below:

$$A(I) \longleftarrow A(I)+B(t)\ (1-\Delta I) \qquad ....(3.4a)$$

$$A(I+1) \longleftarrow A(I+1)+B(t)\ (\Delta I) \qquad ....(3.4b)$$

where A(I) = bin contribution in Ith bin.

and B(t) = the sample value at time t.

We also keep an account of the effective number of samples added in each bin as

$$C(I) \longleftarrow C(I)+(1-\Delta I) \qquad ....(3.5a)$$

$$C(I+1) \longleftarrow C(I+1)+\Delta I \qquad ....(3.5b)$$

where C(I) = the effective number of samples added in Ith bin.

The final average samples, normalized for the system gain, are then obtained as

$$Ave(I) = K.A(I)/C(I) \qquad .....(3.6)$$

where K = system gain normalization factor
= $1/(Dn.G_c)$

Dn = deflection due to the calibration noise

$\propto$ receiver gain

G_c = gain of the correlation beam at the source declination normalized to the gain at zenith.

In the course of this averaging process, if any absolute sample value is found to be greater than 5 times the standard deviation estimated for the data in the respective record, then that sample is rejected as possibly due to interference. However, the bin numbers corresponding to such samples are noted, so that the possibility of these high sample values due to very strong pulses from the pulsar could still be considered, if the bins are found to be confined to the pulse window in the average profiles. The worst case estimate of the standard deviation of the noise in the final profile is obtained as

$$\sigma_T = \left[\frac{\sum_{i=1}^{Nrec} \sigma_i^2}{\sum_{I=0}^{NB-1} C(I).Nrec/NB} \right]^{1/2} \qquad .....(3.7)$$

where σ_T = estimate of the standard deviation of noise in the output profile

σ_i = standard deviation of data in ith record before averaging

and Nrec = number of records used for averaging.

This σ_T is treated as the worst-case estimate, considering the possibility of an over-estimation of σ_i due to the contributions of much slowly varying beam responses of the confusing continuum sources.

In this manner, the average profiles are obtained for both the SIN and COS channels separately.

As the data is averaged over a two-period stretch, each half of the stretch corresponds to average of alternate pulses. These halves can be considered to be two independent sets of data obtained under same observing conditions and to have, in general, same average contribution from the pulsar signal. With this understanding, the data over two-period stretches are tested for significant detection of two similar looking pulses separated exactly by the period of the pulsar. The threshold for the significant detection is chosen to be three times the value of the standard deviation as computed by eq. 3.7 . This procedure increases the reliability of such detections as it can discriminate against the otherwise

possible spurious detections due to interference. However, the signal-to-noise ratio in the two-period stretch is reduced by a factor of $\sqrt{2}$, compared to that in the case of averaging over a one-period stretch, making the detections difficult in the marginal cases. This disadvantage can be overcome by using the data after applying suitable running average over the two-period stretch. It is required that at least one .of the two channels satisfies the detection criterion. It should be noted that, in any further processing, only the original averaged data,for which the running average is not applied, have been used. In the initial stages, in order to comfirm the detections, the corresponding raw data were folded with wrong periodicities and were confirmed to fail in the detection test.

Using the above mentioned procedure, it has been possible to successfully detect signals from 8 pulsars. Their average profiles are obtained by combining the two halves of the two-period stretch for each channel.

To accomplish the above described processing, suitable software programs in Fortran were developed, tested and used on the PDP 11134 and Vax 111780 computer systems at the Raman Research Institute, Bangalore and the Indian Institute of Astrophysics, Kavalur Observatory, respectively. One such output obtained using these programs and the data obtained in the direction of PSR 0834+06, is shown in Fig.3.4.

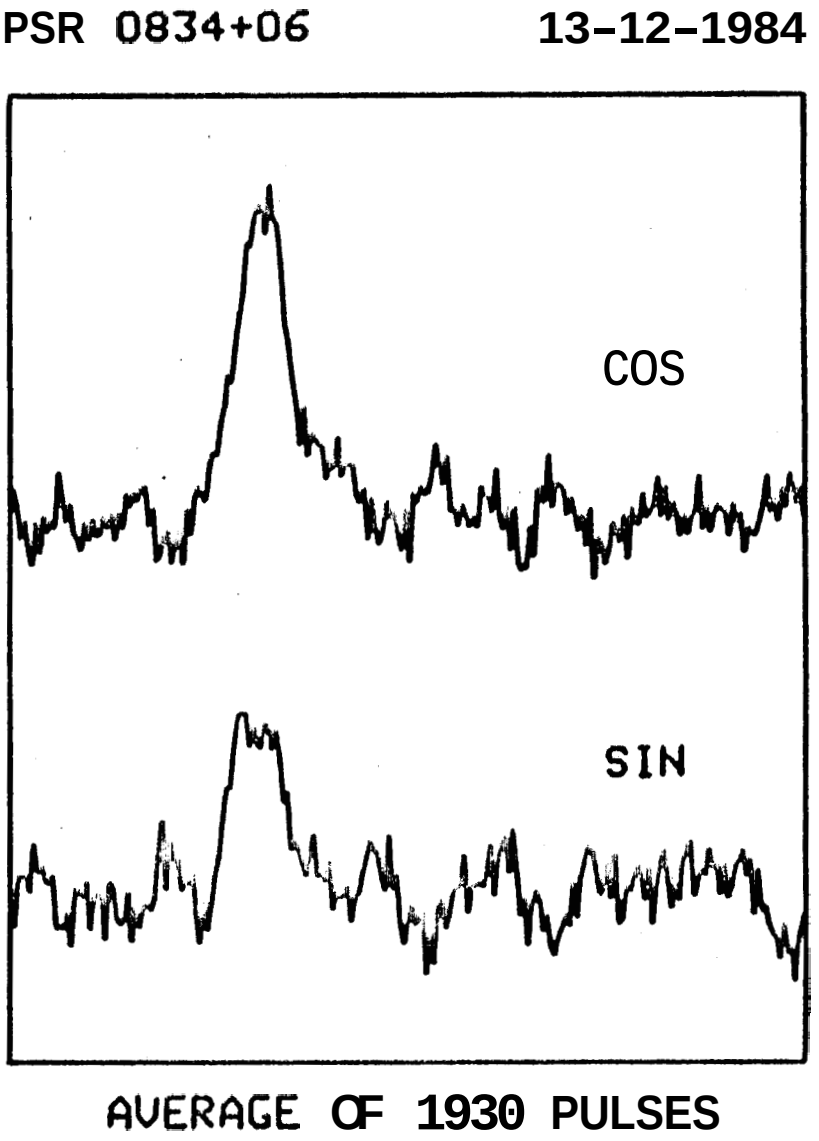

FIG. 3.4 Average profiles in the COS and the SIN channels.

3.2.5 Average Profiles

In the case of each successful detection, the average profiles over a one-period stretch were available for both of the COS and SIN channels. Here we describe the procedure adopted by us to combine the contribution in the two channels. In our case, the COS and the SIN channel outputs (Ac(t) and As(t)) can be written as

$$Ac(t) = g_c\, Ao(t)\, COS(\pi \Delta\theta/\theta_{NS}) \qquad ....(3.8a)$$

$$As(t) = g_c\, Ao(t)\, SIN(\pi \Delta\theta/\theta_{NS}) \qquad ....(3.8b)$$

where g_c = gain factor due to collimation error
= SINC $(\pi \Delta\theta/\theta_{NS})$

θ_{NS} = separation between the peak and the first null of the S arm beam in N-S direction

$\Delta\theta$ = effective collimation error in N-S direction

and Ao(t) = the COS channel output when $\Delta\theta = 0$.

Ao(t), the main function of interest, can be obtained from Ac(t) and As(t) by using the equations (3.8a,b) as

$$Ao(t) = [Ac^2(t) + As^2(t)]^{1/2}/g_c \qquad .....(3.9)$$

The factor g_c can be estimated using the value $\Delta\theta$ obtainable as

$$\Delta\theta = TAN^{-1}[(As(t)/Ac(t)] \cdot \theta_{NS} / \pi \quad ....(3.10)$$

for $Ao(t) \neq 0$

However, in a practical situation ,i.e. in the presence of noise, the signal-to-noise ratio obtainable for Ao(t) is worsened further, if the above procedure is used (see Appendix IV). We present here a new scheme to estimate Ao(t), such that the estimate,in general, will have better signal-to-noise ratio than that available in the individual channels.

In this scheme, the channel, with better signal-to-noise ratio is selected first. As most of the times such a channel corresponds to the COS correlation, for further discussion,we will assume this channel to be the COS channel (Ac(t)). A best fit pulse profile is obtained for this channel data using the minimum χ^2 method. The best fit profile (Fl(t)) takes into account the intrinsic pulse width, dispersion smearing, the receiver time-constant and gives estimates for the pulse amplitude (Ampl) and the amount of the interstellar scattering (τ_s). The best fit profile can be written as

$$Fl(t) = Ampl.g(t) \quad ....(3.11)$$

and

$$g(t) = i(t) * s(t) * d(t) * r(t) \qquad \ldots.(3.12)$$

where $i(t)$ = a gaussian to represent the intrinsic pulse profile.

$s(t)$ = a truncated exponential, with τ_s as the characteristic width representing the scattering in the interstellar medium .

$d(t)$ = the receiver bandpass converted into time function by the dispersion law

$r(t)$ = the impulse response of the post-detection filter.

and $*$ implies convolution

The width of a gaussian pulse in $i(t)$ is obtained using the corresponding value at 400 MHz [94] and assuming that the width $\propto (\text{frequency})^{-0.25}$. The best fit function, $g(t)$, is then used to estimate the best fit pulse amplitude (Amp2) for the other channel output $As(t)$ as,

$$Amp2 = \frac{\int_{0}^{P.N_P} As\,(t)\,dt}{\int_{0}^{P.N_P} As(t).g(t)\,dt} \qquad \ldots.(3.13)$$

The effective collimation error $\Delta\theta$ is then estimated as

$$\Delta\theta = [\text{TAN}^{-1}(\text{Amp2/Ampl})].\theta_{NS} / \pi \quad \ldots.(3.14)$$

Now, it is possible to obtain two independent estimates (say Aol(t) and Ao2(t)) of Ao(t), as follows

$$\text{Aol(t)} = \text{Y.Ac(t)/Ampl} \quad \ldots(3.15a)$$

and $$\text{Ao2(t)} = \text{Y.As(t)/Amp2} \quad \ldots(3.15b)$$

where $$Y = (\text{Ampl}^2 + \text{Amp2}^2)^{1/2}/g_c \quad \ldots.(3.16)$$

The r.m.s. noise deviations ($\sigma 1$, $\sigma 2$) in the profiles Aol(t) and Ao2(t) respectively are given by

$$\sigma 1 = \sigma_T \, Y \, /\text{Ampl} \quad \ldots(3.17a)$$

$$\sigma 2 = \sigma_T \, Y \, /\text{Amp2} \quad \ldots(3.17b)$$

where σ_T = r.m.s. noise deviation in the profile Ac(t), As(t)

It should be noted that the errors in the determination of Ampl and Amp2 are much smaller than σ_T and are therefore ignored here. The two independent estimates, Aol(t) and Ao2(t), are combined with suitable weights, to obtain best possible estimate of Ao(t) using the following equations (see Appendix V)

$$Ao(t) = \frac{Ao1(t).W1 + Ao2(t).W2}{W1 + W2} \quad \ldots.(3.18)$$

where $W1 = (1/\sigma 1)^2$ ...(3.19a)

$W2 = (1/\sigma 2)^2$ ...(3.19a)

As shown in Appendix V , the r.m.s. noise deviation, σo, for the profile Ao(t) is given by

$$\sigma o = \sigma_T / g_c \quad \ldots.(3.20)$$

and the corresponding signal-to-noise ratio is given by

$$(S/N)_{Ao} = (S/N)_{Ac} \left[1+(Amp2/Amp1)^2\right]^{1/2}$$

$$= (S/N)_{As} \left[1+(Amp1/Amp2)^2\right]^{1/2} \quad \ldots.(3.21)$$

where $(S/N)_{Ai}$ = Signal-to-noise ratio for the profile Ai(t)

Thus, by using the above procedure, it is possible to partially recover for loss in signal-to-noise ratio in the COS channel due to collimation errors.

We have used this procedure to obtain the average pulse profiles (Ao(t)) from the COS and SIN channel outputs. Fig. 3.5 shows one such profile obtained for PSR0834+06.

3.3 FLUX CALIBRATION

To obtain appropriate flux calibrations, observations were made on suitable continuum point sources during every session of the pulsar observations. Sources, with declinations close to those of the pulsars observed, were selected for calibration. Table 3.2 lists the calibrators and their assumed fluxes. The assumed flux values at 34.5 MHz for most of these calibrators were obtained by extrapolating from the 38 MHz values [96]. These values were used after applying the correction suggested by Baars et al.[97].

The observations of the calibrating sources were made in the tracking mode and with the single frequency channel analog correlation receiver. The predetection bandwidth was 30 KHz and the post-detection time constant of 1 second was used. The data were sampled and recorded at intervals of 300 milliseconds.

The recorded data during each calibration observation were used to obtain average deflections, Dc and Ds in the COS and SIN channels respectively. The deflection, Do, corrected for collimation error was obtained as :

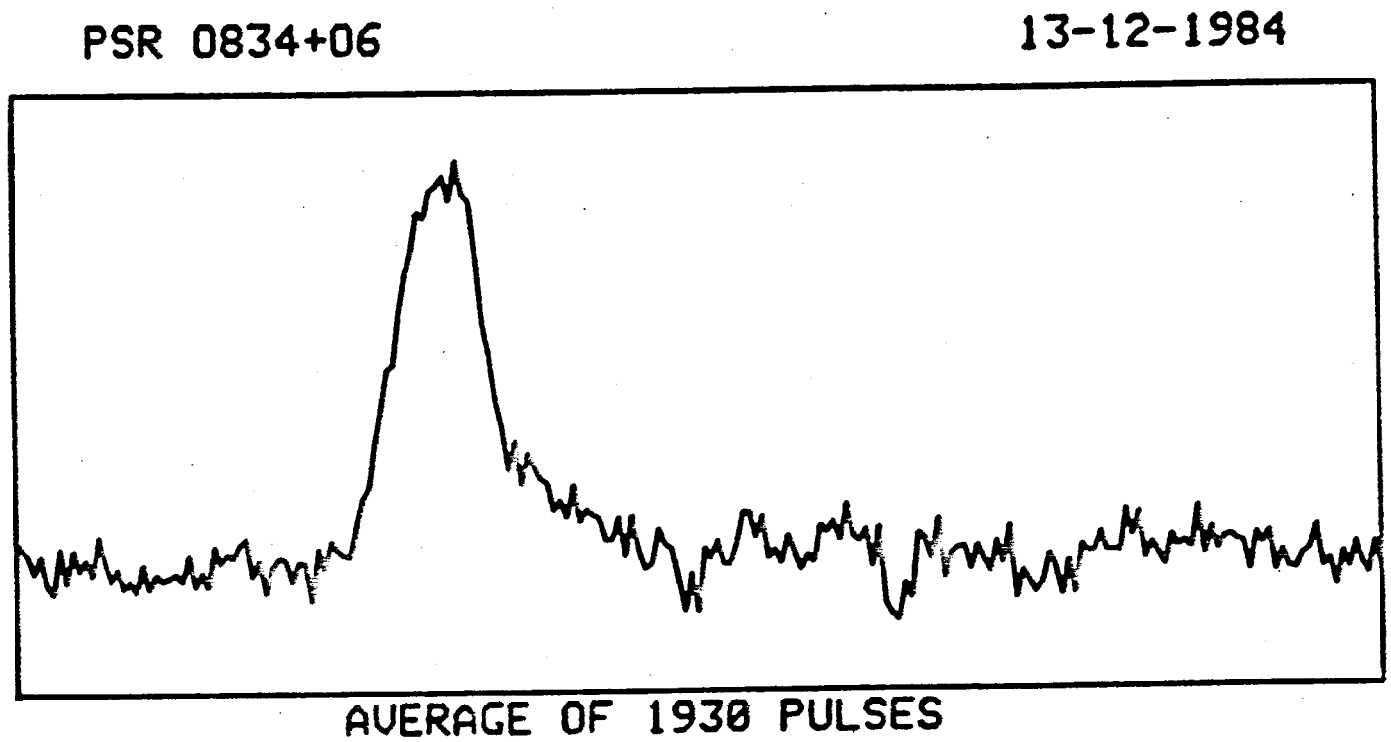

FIG. 3.5 An average profile obtained by combining the COS and SIN channel outputs using the new procedure.

TABLE 3.2 LIST OF CALIBRATION SOURCES AND THEIR ASSUMED FLUXES.

S.No.	Source Name	Assumed flux at 34.5 MHz (in Jansky)	
.1	MSH 00-17	56	
2	3C20	119	
3	3C47	137	
4	3C69	79	
5	3C84	405	
6	3C86	85	
7	3C98	158	
8	3C123	617	
9	MSH 04-218	100	*
10	3C134	354	
11	3C144	2500	
12	3C171	53	
13	3C175	92	
14	3C177	27	
15	3C181	34	
16	3C196	177	
17	3C218	932	
18	3C245	44	
19	3C249	40	
20	3C263	51	
21	3C270	130	
22	3C295	98	
23	3C310	237	
24	3C327	179	
25	MSH 17-211	200	*
26	3C380	234	
27	MSH 22-17	273	*

A extrapolated from the flux at 80 and 160 MHz [95].

$$Do = \frac{(Dc^2 + Ds^2)^{1/2}}{SINC\ [TAN^{-1}(Ds/Dc)]} \qquad ....(3.22)$$

If S is the source strength in Janskys, then the calibration factor Rcal, in Janskys per count of deflection, is given by

$$Rcal = S/(Do.K) \qquad ....(3.23)$$

Such values of Rcal obtained from observations of 5-7 calibrators in each day, were used to obtain an average calibration ‹ Rcal › for the respective day which was used in turn to obtain a calibrated profile, a(t),as

$$a(t)_{(Jansky)} = Ao(t).\langle Rcal \rangle \qquad ....(3.24)$$

3.4 ESTIMATION OF THE AVERAGE PULSE ENERGY AND THE AMOUNT OF INTERSTELLAR SCATTERING

The calibrated average pulse profiles were used to estimate the average pulse energy and the amount of interstellar scattering. For this purpose, a best fit profile was obtained in each case. The nature of the function used to fit the observed profile is as given in eq. 3.12 . The estimate of the average pulse energy was obtained by

integrating the observed pulse profile within the pulse window inferred from the best fit profile.

The calibrated profiles obtained on different days were combined together to improve the signal-to-noise ratios. For the purpose of estimating the average pulse energy, the different days data were averaged with equal weights. The same input data were averaged also with suitable weights (see Appendix V) to maximise the signal-to-noise ratio. This later output was used to obtain the estimates of the amount of interstellar scattering (τ_s). The estimates obtained for 8 pulsars are listed in Table 3.3. Our estimates of τ_s may have larger errors than those quoted here, if our assumptions about the intrinsic pulse profiles ($i(t)$ in eq. 3.12) at 34.5 MHz do not hold good.

3.5 FLUCTUATION SPECTRA

A wide variety of intensity fluctuations are observed from pulsars at high radio-frequencies. Study of such intensity fluctuations in the unexplored low radio-frequency range is of great importance; In this Section, we discuss the possibilities of such a study and report on our attempts in this regard.

TABLE 3.3 ESTIMATES FOR THE AVERAGE PULSE ENERGY AND THE AMOUNT OF SCATTERING AT 34.5 MHz.

S.No.	PSR NAME	Average pulse energy in 10^{-29} $J/m^2/Hz$	Scattering width τ_s in msec
1	PSR 0628-28	1750 ± 480 *	45 ± 15 **
2	PSR 0809+74	710 ± 320	3 ± 2
3	PSR 0834+06	2100 ± 100	16 ± 3
4	PSR 0942-13	110 ± 60	
5	PSR 0943+10	960 ± 120	8 ± 3
6	PSR 0950+08	420 ± 60	9 ± 4
7	PSR 1133+16	900 ± 90	9 ± 3
8	PSR 1919+21	2560 ± 400	

* five sigma error bar

** one sigma error bar

A simple model of the radiation received from pulsars,over a bandwidth much smaller than the center frequency, is that the radiation is white Gaussian noise which is amplitude modulated. We are interested in studying the modulating function and not the noise process. The average nature of this modulating function is studied by measuring the average pulse profiles. The intensity fluctuations can be therefore regarded as the deviations of the modulating function from its average value. The deviations are caused by a variety of processes and can be classified broadly into the fluctuations intrinsic to the pulsar radiation and those due to the intervening medium.

The intrinsic intensity modulation within a pulse period or the pulse structure consists of micropulses, subpulses and average profile in general. The time-resolution obtainable in our case is inadequate for the study related to micropulses. We can, however, attempt to study intrinsic subpulse and average profile fluctuations by obtaining suitable power spectra of the modulation function. Such spectra are known as the fluctuation spectra for pulsars. These spectra can reveal the drifting nature of the subpulses and fluctuations of the pulse energy including the effects of pulse nulling [32,98].

In general, the observed power spectra have contributions due to the fluactuations caused by the intervening medium. It can be shown, that the observed spectrum is a convolution of the spectrum of the intensity modulations due to the invervening medium with the intrinsic modulation spectrum of the pulsar. Thus, if there are any narrow spectral features due to the intrinsic modulation, then they may be smeared due to scintillation in the intervening medium. As the scintillations due to the interstellar medium have very small decorrelation bandwidth (see Appendix II) compared to the observing bandwidth, they can be ignored. The interplanetary and the ionospheric scintillations, however, may be significant. Study of the interplanetary scintillations (IPS) itself may be useful to obtain estimates of unpulsed flux, if any, from pulsars. However, the IPS at low radio frequencies and when observed at low geomagnetic lattitudes is difficult to separate from confusing ionospheric scintillations.

The data obtained on some strong pulsars, from the observations reported in this chapter were analysed using "the longitude-resolved Fourier analysis" method first applied to the study of drifting subpulses by Backer(1970)[98]. In this method, the observed intensities as a function of time at each fixed longitude are Fourier transformed separately. We have chosen the width of the longitude bins, within which the data are averaged, to be 2 percent of the period. A sequence of

samples for a fixed longitude is Fourier transformed in blocks of 256 samples and the amplitude spectra for many blocks are averaged. Such spectra suffer heavily from aliasing effects because a given longitude can provide only one sample per period.

Fig. 3.6 shows the fluctuation spectra versus longitude obtained using the data on PSR0834+06. The values at zero frequency as a function of longitude correspond to the average pulse profile. Such analyses were repeated for this pulsar on different days. At high radio frequncies, the fluctuation spectra for this pulsar show a narrow line feature indicating strong periodic modulation at about 0.46 cycles/period [27]. However, at our frequency, the spectra for longitudes within the pulse window do not show any' significant deviation from those for longitudes outside the pulse window. Our observations suggest that any periodic modulation which can result in a narrow line feature must be weak at 34.5 MHz and that the depth of modulation does not exceed 6 percent, when it would have been seen above the noise. It is possible that there is strong modulation, but then its contribution must be spread over a broad region in the spectrum.

3.6 LOW FREQUENCY VARIABILITY

Variability in the received flux from pulsars has been extensively studied at high radio-frequencies (e.g.[99]).

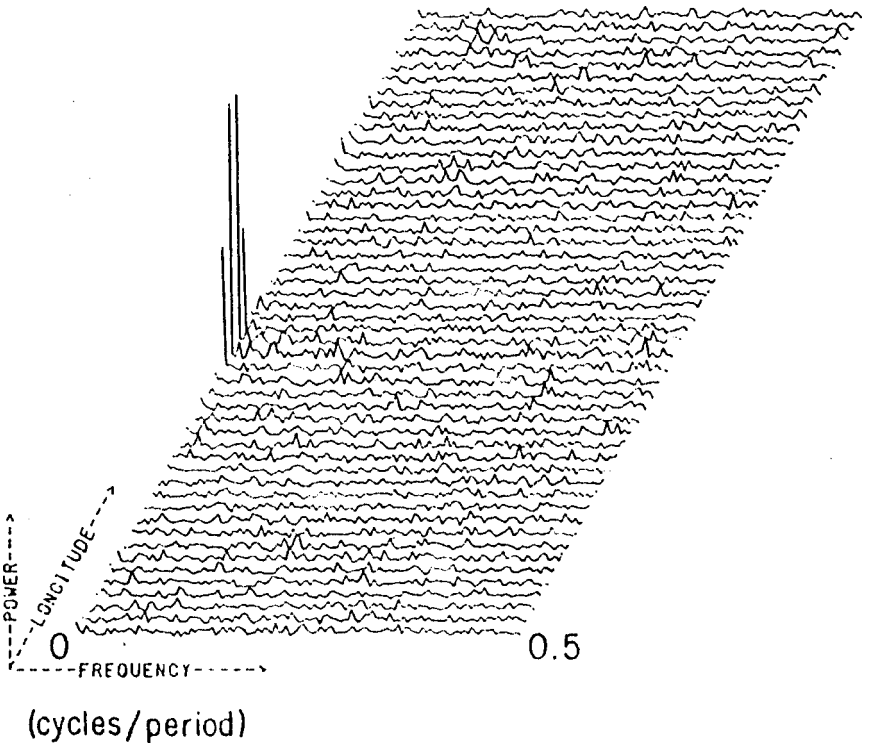

FIG. 3.6 Fluctuation spectra Vs. longitude for PSR 0834 +*06* at 34.5 MHz.

These flux variations have time scales in a wide range. The slow variability is generally attributed to the refractive scintillations produced by large size density irregulatiries in the interstellar medium [100]. No measurement of such variability at decametric wavelengths has been reported so far in the literature.

We have made some attempts to make such measurements using the single frequency-channel observations discussed in this chapter. For this purpose we have selected three strong pulsars and have made observation on them on different days spaning over 80 days. The calibrated pulse energies obtained from these observations have been used to compute a modulation index , $\bar{m}$, as defined by Slee et al.[64].

$$\bar{m} = \left[\sum_{i=1}^{n_o} (Si - \bar{S})^2 / n_o \right]^{1/2} (\bar{S})^{-1} \quad ....(3.25)$$

where Si = the measured value of the pulse energy in the i th observation

n_o = number of observations

and $\bar{S} = \sum_{i=1}^{n_o} Si/n_o$

The computed modulation indices in two of the three cases, did not indicate any significant modulation other than the apparent modulation caused due to the errors in calibration f'rom day to day. Only in the case of PSR 0950+08 , we find significant modulation. The estimated value of $\bar{m}$, in this case, is **0.34** 20.15 . The large error in the estimate is mainly attributed to the calibration errors. Further observations over longer time spans can be undertaken for **detailed investigation.**